Figures

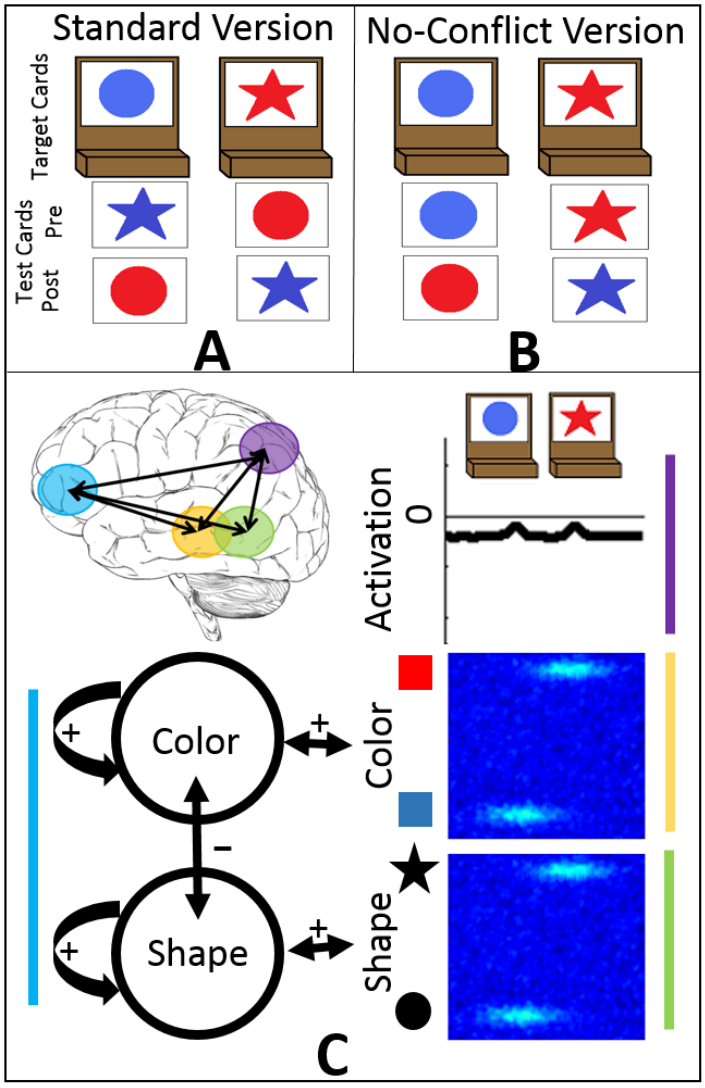

Figure 1 | **Dimensional Change Card Sort Task and Dynamic Neural Field Model** Panel A shows the sorting trays, test cards and target cards typically used in the Standard DCCS task. Panel B shows the trays, test cards and target cards typically used in the No-Conflict version of the DCCS. Panel C shows the DNF model architecture and mapping to cortical regions (see colors on brain inset and vertical colored bars next to the model architecture). The model has task inputs corresponding to the spatial locations and visual features present on the target cards.

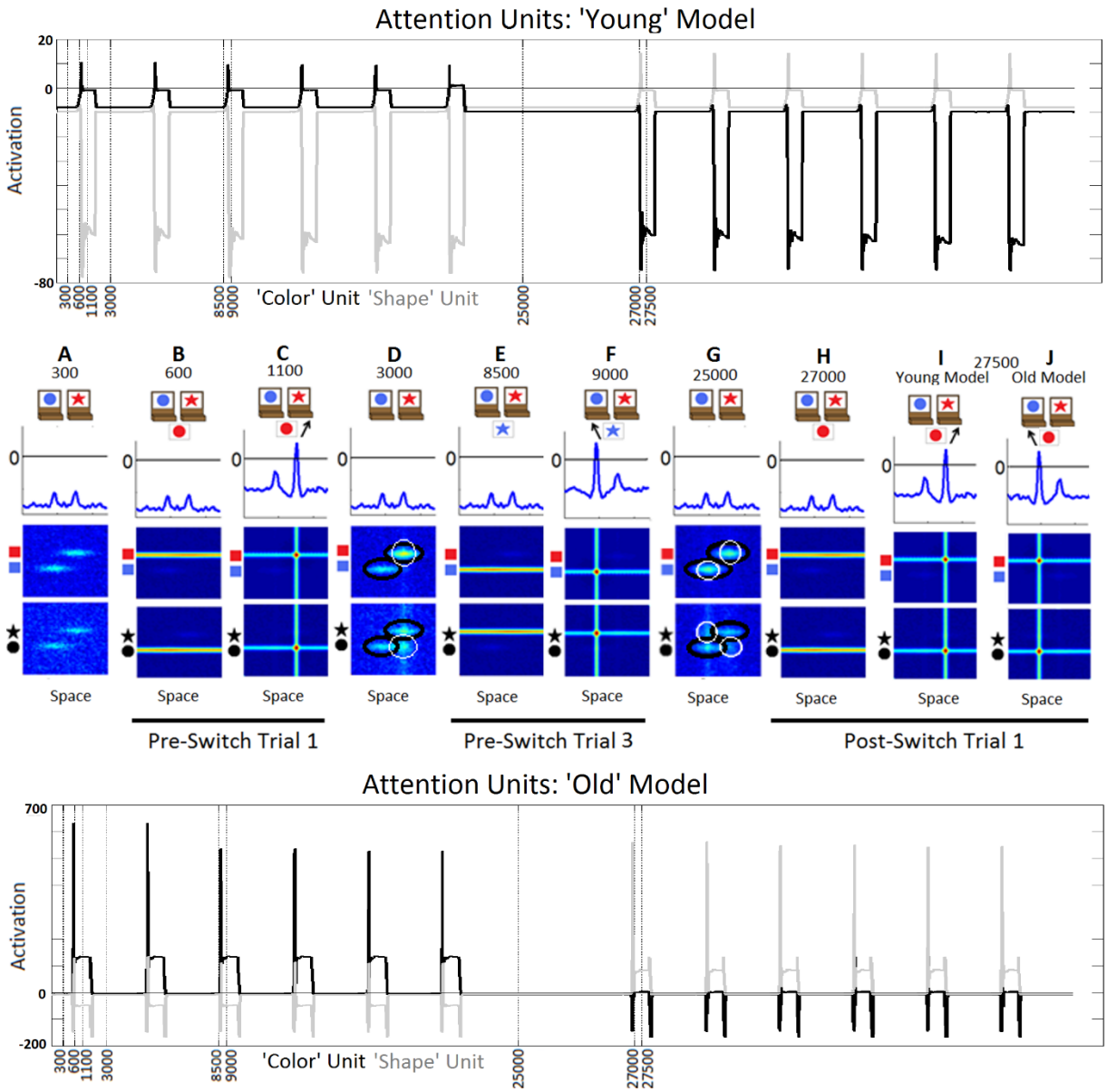

Figure 2 | Model performing the DCCS task The top and bottom panels show the activation of the attention units in the frontal component over the course of the pre- and post-switch phases. Panels A-J show images of the parietal and temporal components at different time points. Panel A shows the model with the inputs for the target cards and sorting trays. Panel B shows the model just after the first test card has been presented to the model. Panel C shows the model making a sorting decision on the first trial. Panel D shows the model with the memory traces accumulated during the first trial. Panel E shows the model just after the third pre-switch test card has been presented. Panel F shows the model making a sorting decision during the third pre-switch trial. Panel G highlights the configuration of test inputs and memory traces just before the start of the post-switch phase. Panel H shows the model just after the first post-switch test card has been presented. Panel I shows the 'young' model perseverating during the first post-switch trial. Panel J shows the 'old' model correctly switching rules during the first post-switch trial.

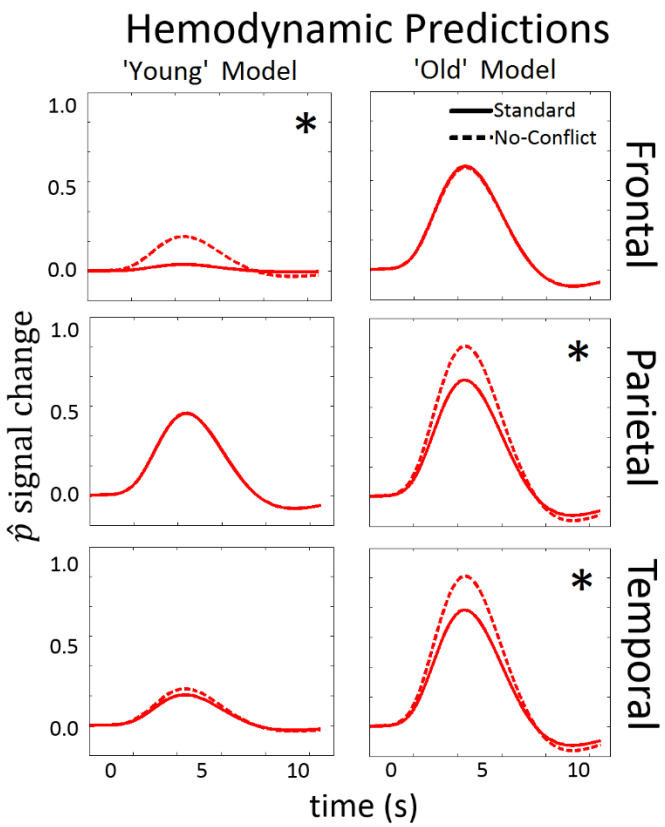

Figure 3 | Hemodynamic predictions from the DNF models The model makes a pattern of hemodynamic predictions from the frontal (top), parietal (middle) and temporal (bottom) components of the DNF model. Asterisks mark components that show a significant difference in activation between conditions.

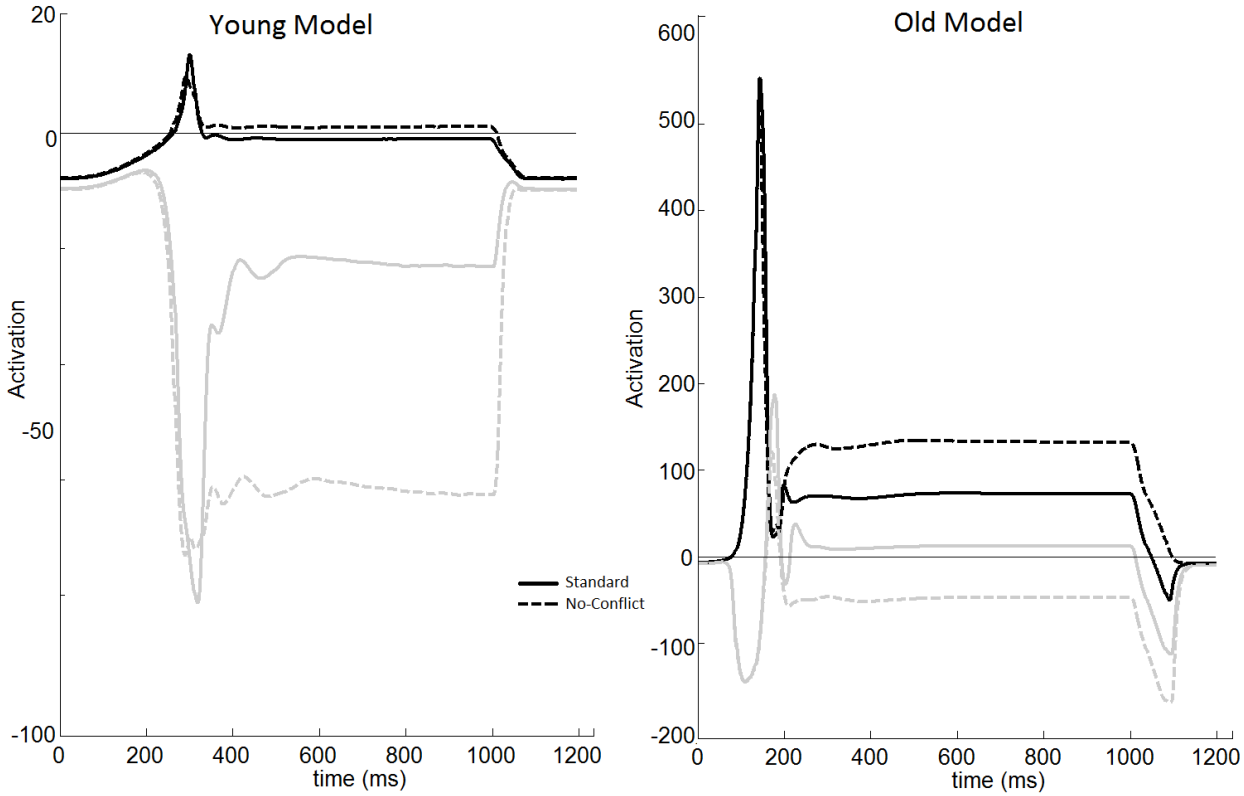

Figure 4 | Activation of Dimensional Nodes The dimensional nodes are plotted for the 'young' and 'old' model in post-switch trials for the Standard and No-Conflict conditions (the relevant dimensional node is plotted in black, the irrelevant dimensional node is plotted in grey). For the 'young' model, the relevant dimensional node becomes activated above threshold in the No-Conflict condition but not in the Standard condition (i.e., between 400 and 1000 ms). For the 'old' model, the relevant dimensional node becomes more robustly and stably active in the No-Conflict condition relative to the Standard condition (i.e., between 200 and 1000 ms).

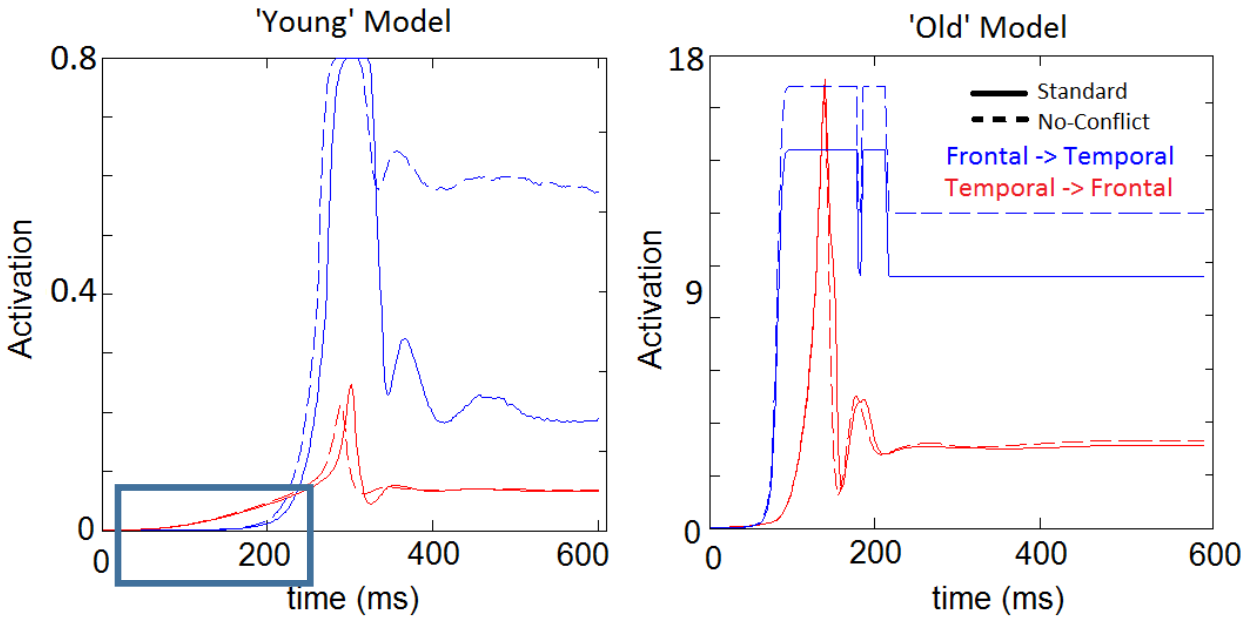

Figure 5 | Frontal-Temporal Interactions Activation strengths between the frontal and temporal components are plotted for the 'young' and 'old' model in post-switch trials during the Standard and No-Conflict conditions. For the 'young' model, activation along the temporal-to-frontal connection begins before the activation along the frontal-to-temporal connection. Additionally, activation in the No-Conflict condition peaks before activation in the Standard condition. For the 'old' model, activation along the frontal-to-temporal connection begins before activation along the temporal-to-frontal connection. Additionally, activation along the frontal-to-temporal connection is stronger in the No-Conflict condition than in the Standard condition.

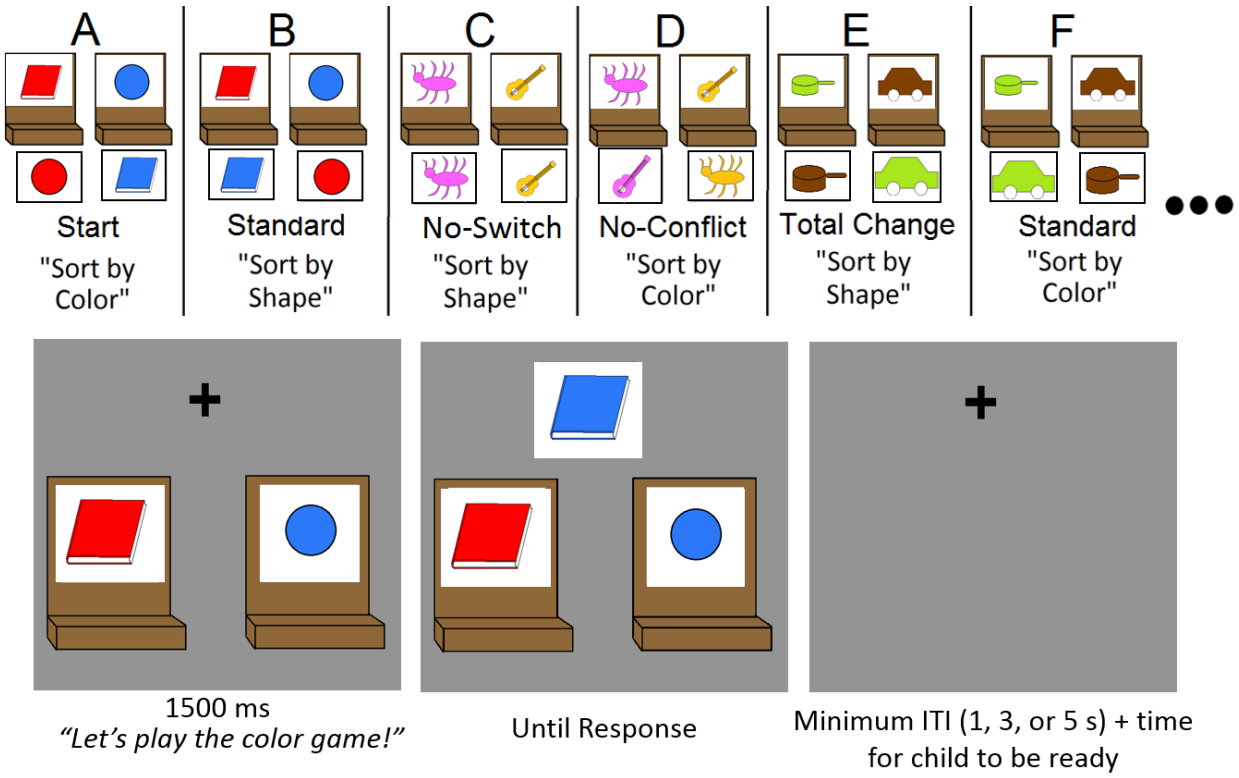

Figure 6 | Behavioral Task Top panel shows example sequence of sorting phases. Each phase contained 3 trials. Panel B shows the switch phase for the Standard condition. Here, the relevant dimension has changed from the previous phase in Panel A and the features have all remained the same so that the test cards need to be sorted to different locations between A and B. Panel D shows the No-Conflict switch condition. As with the Standard condition, the relevant dimension has changed. The just previous phase in Panel C contained no-conflict cards. Thus, the transition from Panel C to Panel D characterizes the No-Conflict condition as illustrated in Figure 1B. Panel C shows the No-Switch condition (which serves as the pre-switch phase for the No—Conflict condition. The bottom panel shows the sequence of events on each trial.

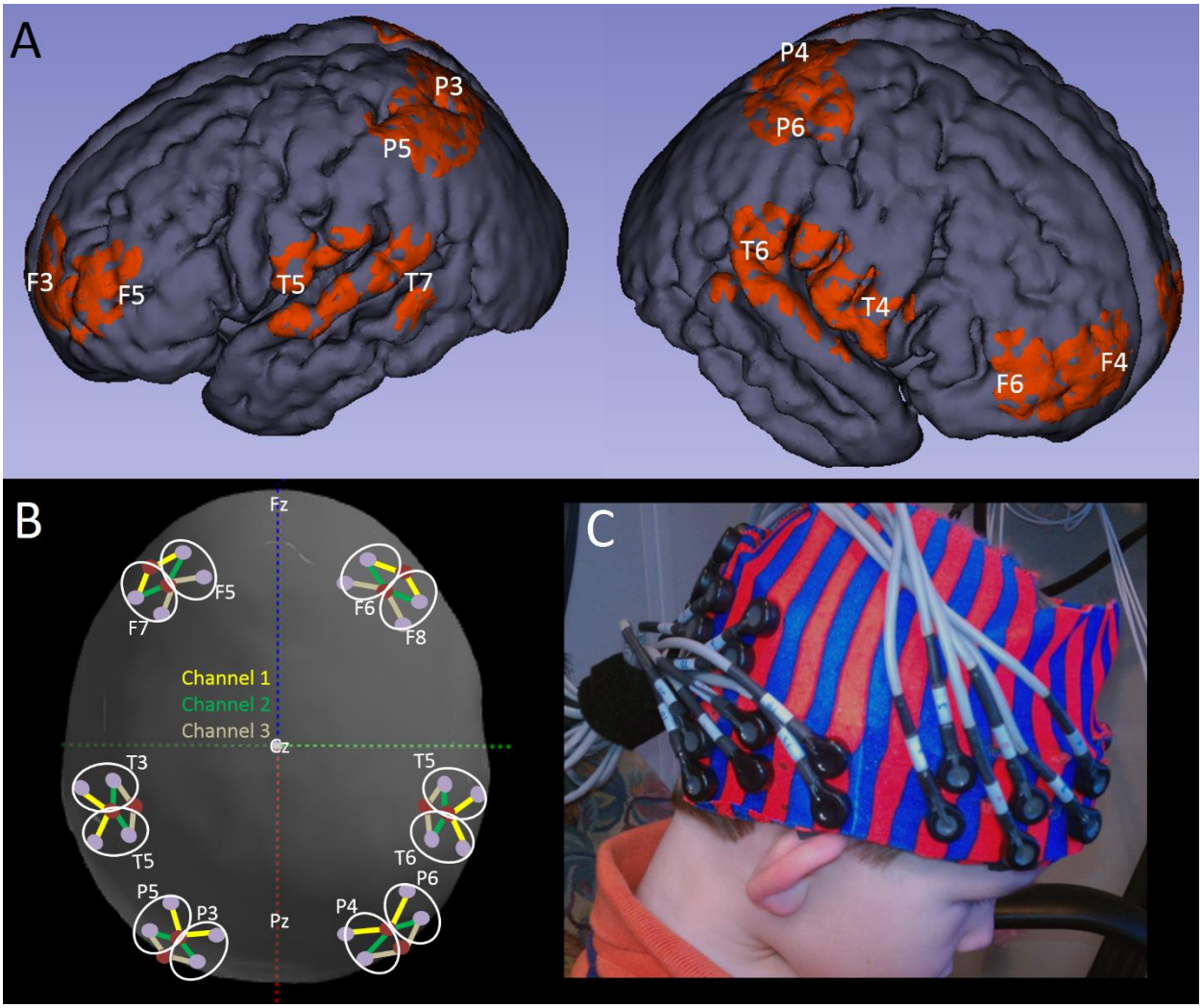

Figure 7 | fNIRS Probe (A) shows a digital projection of the fNIRS probe onto a standard brain atlas. (B) Shows the numbering scheme for the channels at each region (see Table 1). (C) Shows a photo of a participant wearing the fNIRS probe.

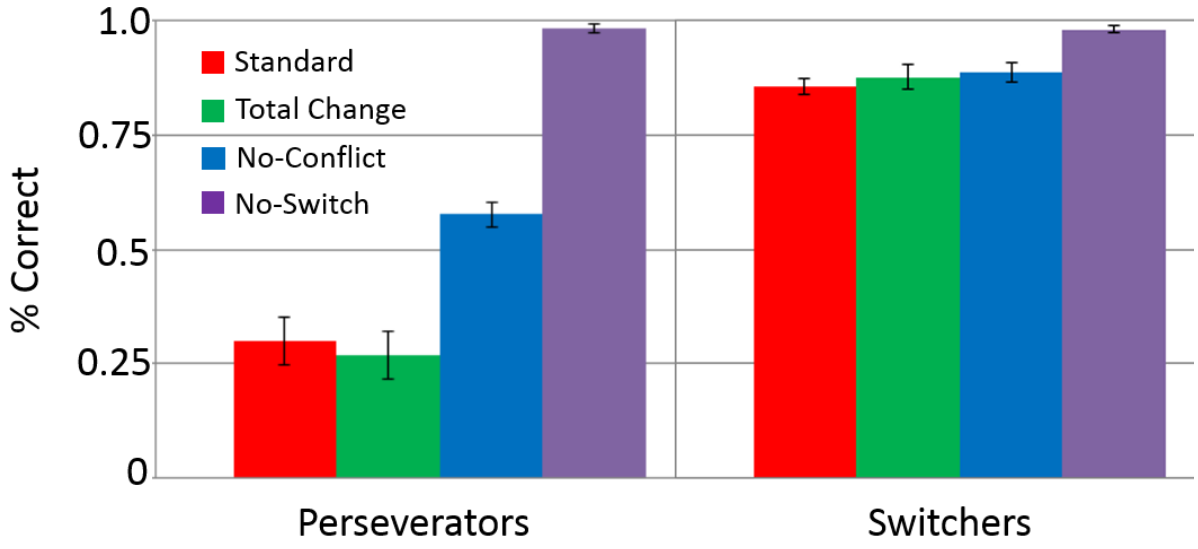

Figure 8 | Behavioral Results Average percent correct across conditions for valid switch trials. Error bars represent standard error of the mean.

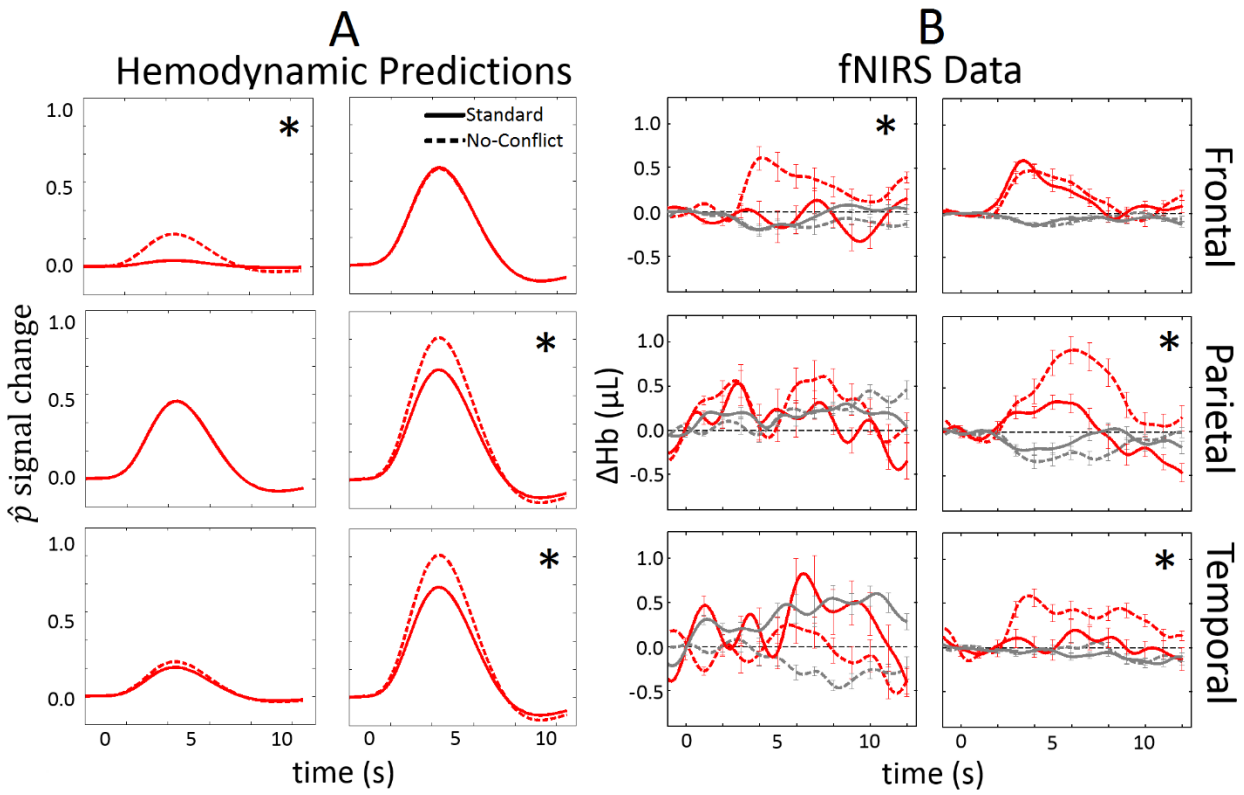

Figure 9 | fNIRS Results (A) Reproduction of the hemodynamic predictions of the DNF model from Figure 3. (B) Group average hemodynamic response for the time-window from 1 second before the onset of a trial up to 12 s post onset of a trial. Oxy-Hb data are plotted in red and Deoxy-Hb data are plotted in gray. Oxy- and Deoxy-Hb data were averaged from a time window spanning 2 s post stimulus to 10 s post stimulus for ANOVA analyses. Asterisks mark regions that showed a significant Oxy x Condition interactions in the ANOVA.